

Active Tectonics and Erosional Unloading at the Eastern Margin of the Tibetan Plateau

Alexander L. Densmore

Institute of Geology, Department of Earth Sciences, ETH Zentrum, CH-8092 Zürich, Switzerland

Email: densmore@erdw.ethz.ch

LI Yong

National Key Laboratory of Oil and Gas Reservoir Geology and Exploitation, Chengdu University of Technology, Chengdu 610059, China

Email: liy@cdut.edu.cn

Michael A. Ellis

Center for Earthquake Research and Information, University of Memphis, 3890 Central Avenue, Memphis, TN 38152, USA

ZHOU Rongjun

Institute of Earthquake Engineering, Seismological Bureau of Sichuan Province, Chengdu 610041, China

Abstract: The eastern margin of the Tibetan Plateau is marked by an extremely steep mountain front with relief of over 5 km. This topography, coupled with abundant Mesozoic thrusts within the margin, explains why tectonic maps of the India-Asia collision typically show the eastern margin as a major thrust zone. Actually, it does not like that. Field observations suggest that the margin is better characterized as a zone of NNE-directed dextral shear with extensive strike-slip faulting and secondary thrusting. The high relief and steep gradients are partially explained by erosional unloading of an elastic lithosphere; the pre-erosion inherited topography may be the inherited Mesozoic thrust belt landscape modified by a component of Cenozoic tectonic shortening.

Keywords: Tibetan Plateau; tectonic; erosional unloading; faulting

Introduction

The eastern margin of the Tibetan Plateau, adjacent to the Sichuan Basin (Figure 1), has become a testing ground for a variety of models that contrast mechanisms of extrusion and crustal thickening associated with the India-Asia collision (Avouac and Tapponnier 1993, England and Houseman 1986), but that also address the extent to which the upper crust and upper mantle are coupled (Royden *et al.* 1997, Holt 2000). The margin is characterized by topographic relief of over 5 km and by the steepest gradient of any edges of the plateau. In large part for these reasons, the eastern margin, which we refer to here as the Longmen Mountains region for convenience, is typically identified on tectonic maps as a major thrust zone.

Evidence for active thrusting, however, is

Received: 15 March 2005

Accepted: 10 May 2005

sparse and equivocal (CHEN *et al.* 1994, Burchfiel *et al.* 1995, Kirby *et al.* 2000), and geodetic surveys constrain active shortening in the Longmen Shan to $0 \pm 5 \text{ mm y}^{-1}$ relative to the Sichuan Basin (King *et al.* 1997). The lack of a late Cenozoic foreland basin adjacent to the margin is also inconsistent with major thrusting in the margin ranges (Burchfiel *et al.* 1995).

The origin of the topography and relief in the Longmen Shan region has been attributed to lateral expulsion of a fluid lower crust from beneath Tibet (Royden *et al.* 1997, Clark and Royden 2000), a

mechanism of mountain building that does not require crustal scale faults but which is potentially inconsistent with seismic measurements in southern Tibet that support coupled upper crust and upper mantle (Holt 2000). Adding to this, the apparent paucity of active faulting and the role of the region in the India-Asia collision are largely enigmatic.

What we describe here is the new evidence for active faulting within the Longmen Shan region, added to the process of erosional unloading, which may help resolve the enigma.

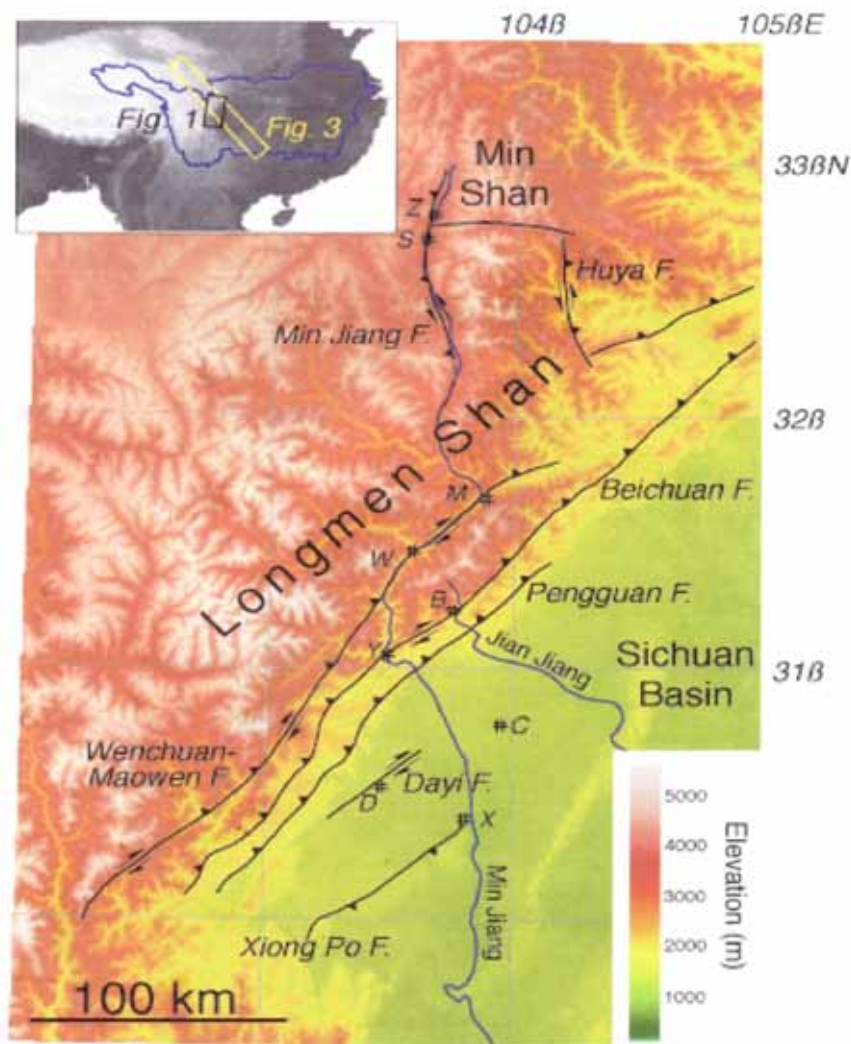


Figure 1 Topography of eastern Tibetan plateau from USGS HYDRO1k elevation data, with 1 km cell spacing. Inset shows the locations of Figure 1 and 3 (boxes) as well as the outline of the Yangtze River drainage basin, which sets local base level for the rivers draining the margin. Faults are shown by black lines; thrust faults have teeth on the hanging wall. Note the correspondence between large strike-slip faults and major northeast-trending valleys. B-Baishuihe; C-Chengdu; D-Dayi; M-Maowen; S-Songpan; W-Wenchuan; X-Xinjin; Z-Zhangla.

1 Geological Background

The structure of the Longmen Shan region is dominated by northeast-trending thrusts and overturned folds that verge to the east and southeast (Burchfiel *et al.* 1995, CHEN and Wilson 1996). Crustal shortening occurred from the late Triassic period to early Jurassic period and again in the late Cretaceous period (Dirks *et al.* 1994). Burchfiel *et al.* (1995) recognized at least four distance phases of Cenozoic deformation within the region. Their final phase, post-Oligocene (post-Miocene?) in age, involved oblique dextral-reverse motion on the Wenchuan-Maowen, Beichuan, and Pengguan faults, reverse and possibly sinistral motion on the Minjiang River faults, and thrusting and folding within the western Sichuan Basin (Figure 1). They noted, however, that the firm evidence for Quaternary displacements was difficult to find, largely because of the scarcity of well-dated Neocene and Quaternary sediments. Major faults in the region are coincident with the main river valleys and the areas of highest relief, suggesting that fluvial erosion has been concentrated along pre-existing geological structures.

2 Observations of Active Faulting

We mapped Quaternary faults on the basis of geomorphic evidence in both the easternmost Tibetan Plateau and the western Sichuan Basin. Age constraints on faulted deposits and landforms are generally poor, so we focus on the kinematics and distribution of active faults, rather than on slip rates.

2.1 Minjiang fault

Burchfiel *et al.* (1995) suggested that the Minjiang fault accommodated E-W Tertiary shortening, with only a minor sinistral component. Kirby *et al.* (2000) cited undeformed Holocene terraces as evidence that the late Quaternary slip rate on the Minjiang fault was $<1 \text{ mm y}^{-1}$.

A prominent ridge 1 km west of the village of Zhangla (Figure 1) is sinistrally offset by a strand of

the Minjiang fault that trends 014. The ridge crest appears unmodified by fluvial incision from either side or by mass wasting. Its age is unknown, but our measured offsets (Figure 2C, 2D) yield a strike-slip ratio of $\sim 2.7:1$.

Approximately 2 km south of Zhangla, a separate strand of the Minjiang fault is visible as a low scarp (east side up) that trends 045 across a fill terrace on the east bank of the Min River (Figure 2E). A well-defined sag pond (50 m long, 0.75 m deep) at a 5° bend in the fault implies a sinistral slip component. Kirby *et al.* (2000) estimated the age of the fill terrace as between 14 and 6.6ky. The pristine appearance of the scarp and sag pond in unconsolidated terrace material argues strongly for Holocene activity along this fault strand. Taken together, these observations are consistent with active sinistral displacement on the Minjiang fault, with a secondary thrust component.

2.2 Wenchuan-Maowen fault

The active trace of the Wenchuan-Maowen fault is best exposed along a 5 km segment just south of the town of Maowen (Figure 1). The fault forms a 4.5 m scarp (east side up) trending 060 across a fill terrace 140 m above the modern Min River. No horizontal offset of the terrace surface was observed, but the fault offsets a ridge crest which bounds the southwest side of the terrace by ~ 50 m dextrally and vertically (east side up). No reliable age for the fill terrace exists, although a sandstone cobble from 2 m below the terrace surface has yielded an electron spin resonance (ESR) age of 161 ky. The fault can be traced for ~ 1 km north of the terrace as a low (<0.5 m), poorly defined scarp across the heavily cultivated floodplain of the Min River. A second, possibly collinear strand of the Wenchuan-Maowen fault is expressed as a 1.0 m scarp (west side up) that trends 060 across the lowest fill terrace of the Min River at the southern edge of Maowen, 4 m above the modern river level. This strand may be traced for ~ 2 km southwest from Maowen before becoming obscured by recent construction work.

2.3 Beichuan fault

2 km north of the town of Baishuihe, a strand

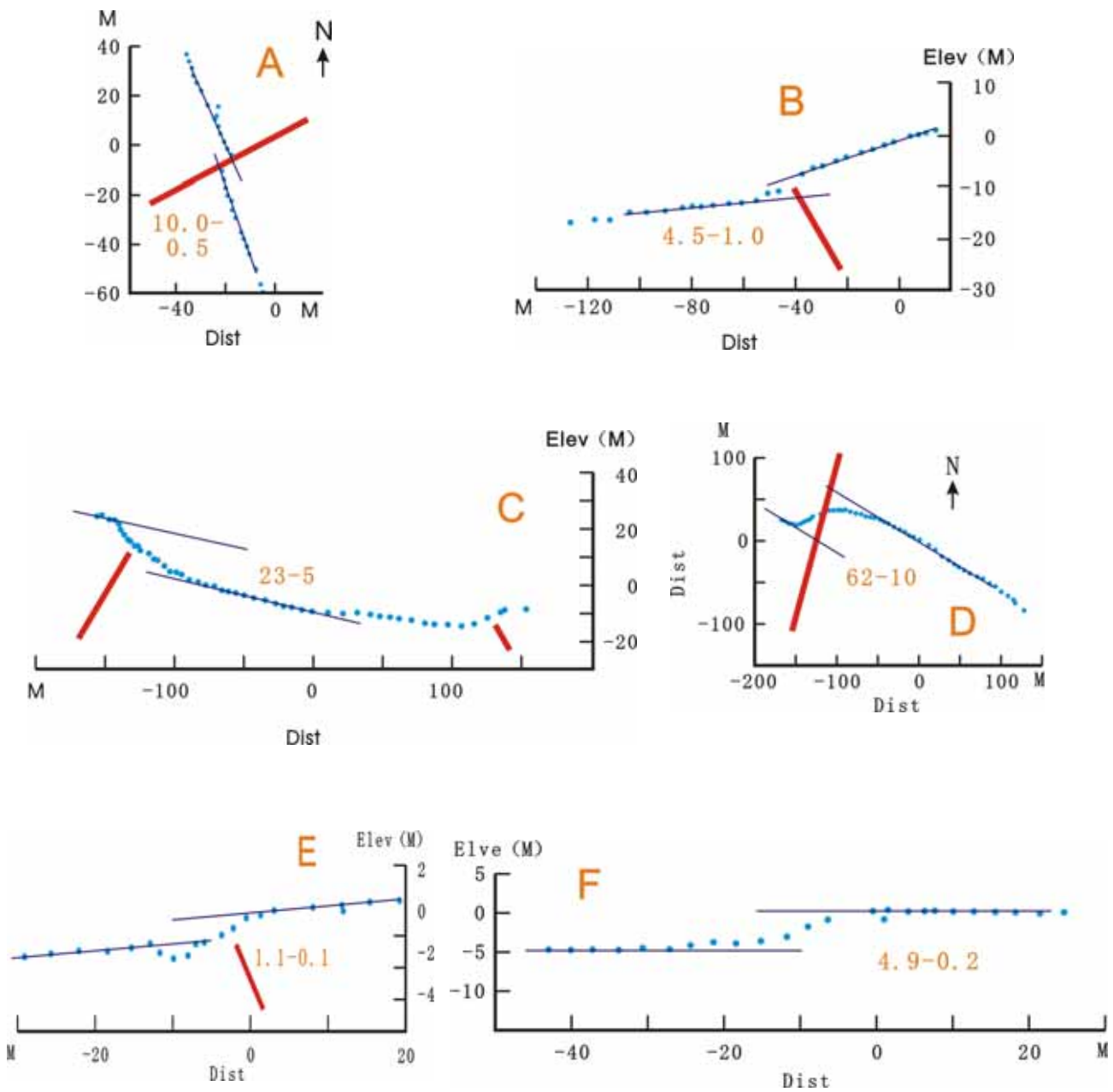


Figure 2 Surveys of offset Quaternary deposits along major the faults in the Longmen Shan region. Fault traces are shown by grey bars. All scales are in meters, and origins and datums are arbitrary. Cross sections are shown at 2x vertical exaggeration. N-northing; E-easting; Dist-fault-perpendicular distance; Elev-elevation.

- A, plan view of gully wall offset dextrally 10.0 ± 0.5 m by Beichuan fault near Baishuihe.
- B, cross section of fill terrace offset 4.5 ± 1.0 m by Beichuan fault near Baishuihe.
- C, cross section of ridge crest offset 23 ± 5 m by strand of the Minjiang fault, 1km west of Zhangla.
- D, plan view of ridge crest shown in C. Crest is offset sinistrally 62 ± 10 m.
- E, cross section of fill terrace offset 1.1 ± 0.1 m by strand of the Minjiang fault, 2 km south of Zhangla. Note the 0.75 m deep sag pond at base of scarp, associated with sinistral displacement along a 5° left bend in the fault.
- F, cross section of floodplain offset 4.9 ± 0.2 m by the Xiong Po fault, 5 km south of Xinjin.

of the Beichuan fault forms a 4.5 m scarp (west side up) trending 068 across a fill terrace 60 m above the modern Jian Jiang (Figure 1, Figure 2B). The fault can be traced for ~2 km to the northeast and separates sheared, locally mylonitic granitic bedrock from clayey sands and gravels of the terrace deposit. We suspect, but cannot prove, that the bedrock has been thrust over the terrace deposit. However, there is abundant geomorphic evidence for Quaternary activity on the fault, including fault-controlled saddles, dextral shutter ridges and dextral channel offsets (Figure 2A).

We interpret the Beichuan fault as an active dextral-slip fault with a thrust component and a probably strike-slip to dip-slip ratio of ~2:1. A sandstone cobble from 2 m below the top of the fill terrace deposit has yielded an ESR age of 57 ky. The dextrally offset channel in Figure 2A is cut into colluvium that locally drapes the fill terrace and is thus younger than the terrace deposit.

The active strand of the Beichuan fault can be traced on Landsat 7 imagery southwest to Yingxiu (Figure 1), where the fault forms a 2.5 m deep graben across a strath terrace 50 m above the modern Min River.

2.4 Pengguan fault

2 km north of the village of Tongjichang, the Pengguan fault forms a 2.5 m scarp (west side up) trending 040 across a fill terrace 30 m above the modern Jian River (Figure 1). Silty sand taken from 1.5 m below the terrace surface has yielded a thermoluminescence age of 22.3 ± 1.8 ky, suggesting the latest Quaternary fault activity. The fault does not offset the floodplain of the Jian River, but is clearly visible ~3 km southwest of Tongjichang as a series of aligned saddles and dextrally offset ridges. Nearby minor brittle faults in Triassic shales are oriented 030/90, subparallel to the Pengguan fault, and show slickensides that trend 210/20, consistent with dextral displacement with a dip-slip component (west side up) and a strike-slip to dip-slip ratio of ~2-3:1.

2.5 Dayi fault

The subvertical Dayi fault can be traced as a series of low scarps and pressure ridges in

Quaternary deposits along the western edge of the Sichuan Basin (Figure 1). At the village of Daomingchang, 9.8 km northeast of Dayi, the fault forms two elongate, en echelon ridges, 15 m wide and 3 m high, that trend 030 and fold unconsolidated red clayey sands with minor gravel lenses. We interpret these as pressure ridges indicating Quaternary dextral displacement on the Dayi fault, which strikes 050~060. The fault does not define the mountain front, which is locally low (<1000 m of relief) and is likely due to contrasts in erodibility between Eocene and Quaternary rocks.

Dip-slip displacement on the Dayi fault is only locally observed and appears relatively minor. At Dongguan, 6 km northeast of Dayi, the fault forms a 1.5 m scarp (west side up) trending 050 in Quaternary (probably Holocene) floodplain deposits, 5 m above the level of the local tributary to the Min River.

2.6 Xiong Po fault

The Quaternary deposits of the western Sichuan Basin are ponded against several elongate and partially fault-bounded anticlines that fold upper Triassic to Cretaceous rocks (Burchfiel *et al.* 1995). At the village of Huangtupo, deeply weathered red Cretaceous sandstone is thrust over matrix-supported yellow silt with scattered sandstone clasts. The thrust plane is oriented 035/60S and is expressed as a zone of intense brittle shearing and shattered clasts. The silt has yielded a thermoluminescence age of 120 ky. We interpret the thrust as the surface expression of an active strand of the fault underlying the Xiong Po anticline, here termed the Xiong Po fault (Figure 1).

5 km south of the town of Xinjin, the Xiong Po fault forms a 4.9 m scarp (east side up) trending 055 across Quaternary (probably Holocene) floodplain sediments of the Pu River, a tributary to the Min River (Figure 1, Figure 2F). Cretaceous shale and fine sandstone in the hanging wall block steepen from 064/38N to 064/65N toward the fault trace. Taken together, the exposure of the Xiong Po fault indicates Quaternary thrust displacement, well to the east of the present Sichuan Basin margin.

Active fault kinematics in the Longmen Shan region suggest that the eastern Tibetan Plateau

margin is deforming over a wide (~200 km) zone of NNE-directed dextral shear, consistent with some models of the India-Asia collision (e.g., England and Molnar 1990). However, this does not explain the presence of the abrupt topographic escarpment at the margin in the absence of major shortening. Below, we test the hypothesis that some of the escarpment relief is due to the effects of erosional unloading and subsequent rock uplift.

3 Topographic Profiles

To assess the large-scale morphology of the region, we constructed profiles of maximum, minimum, and mean elevations across a 1700 by 250 km swath using USGS HYDRO1 k elevation data (Figure 3A). Maximum and mean profiles show the distinction between plateau and basin, and importantly also show that both the basin and the easternmost ranges tilt away from the margin. This tilt is consistent with the virtual absence of the late Cenozoic sediments within the basin. The minimum profile illustrates the elevations of the river system that drains the region, and demonstrates that base level for the system is controlled by the Yangtze River, well to the east of the margin. The maximum profile shows a raised lip at the edge of the plateau, a form characteristic of flexural deformation and observed in many tectonically active ranges (e.g., Stein *et al.* 1988, King and Ellis 1990).

4 Erosional Unloading and Flexural Deflection

Erosion results in a negative load on the lithosphere as crustal rocks are replaced by air. Assuming that most of the present topography was created by incision into a preexisting, low-relief landscape (WANG *et al.* 1998, Kirby *et al.* 2000), we take the negative erosional load to be the depth of dissection, defined as the difference between maximum and mean elevations at each point along the swath (Gilchrist *et al.* 1994). To this negative load we add a small positive load due to the thin (<400 m) Quaternary sediments at the western margin of the Sichuan Basin (Burchfiel *et al.* 1995). We model the lithosphere as an elastic beam of

specified density and effective elastic thickness, T_e overlying a viscous substrate. Deviatoric stresses in the viscous layer are implicitly assumed to relax over a short time scale compared to the duration of unloading. We calculate deflections using the general solution to the flexure equation for an individual line load (Hetenyi 1974):

$$w = \frac{H}{2a(p_m - p_a)g} \exp\left(-\frac{x}{a}\right) \left[\cos \frac{x}{a} + \sin \frac{x}{a} \right]$$

w is the flexural deflection;

H is the magnitude of the load (as force per unit length);

p_m is the mantle density (3300 kg m⁻³);

p_a is the air density (1 kg m⁻³);

g is gravitational acceleration (9.8 m s⁻²);

x is the horizontal distance from the load;

a is the flexural parameter depending on T_e .

There is little constraint on our choice of T_e , so we calculate deflection profiles for a likely range of T_e between 5 and 25 km (McKenzie and Fairhead 1997, Maggi *et al.* 2000), and we take $T_e=15$ km as a reasonable average.

5 Results

Deflection profiles for different values of T_e show similar long wavelength patterns, with maximum deflection adjacent to the plateau margin (Figure 3B). We reconstruct the assumed pre-erosion topography by subtracting the deflection profile for $T_e=15$ km from the present maximum topography (Figure 3C). The reconstructed topography slopes more gently from the plateau to the Sichuan Basin than does the present margin. We interpret the reconstructed topography as the sum of the inherited, pre-erosional landscape plus a syn-erosional tectonic component related to the India-Asia collision. In support of this, we note that the reconstructed Sichuan Basin strongly resembles a typical flexural foreland basin, with a foredeep at the margin and a forebulge at ~910 km, 75 km forward of the margin (Figure 3C). Erosionally-driven flexure of the margin has lifted and tilted the foredeep to the southeast, so that

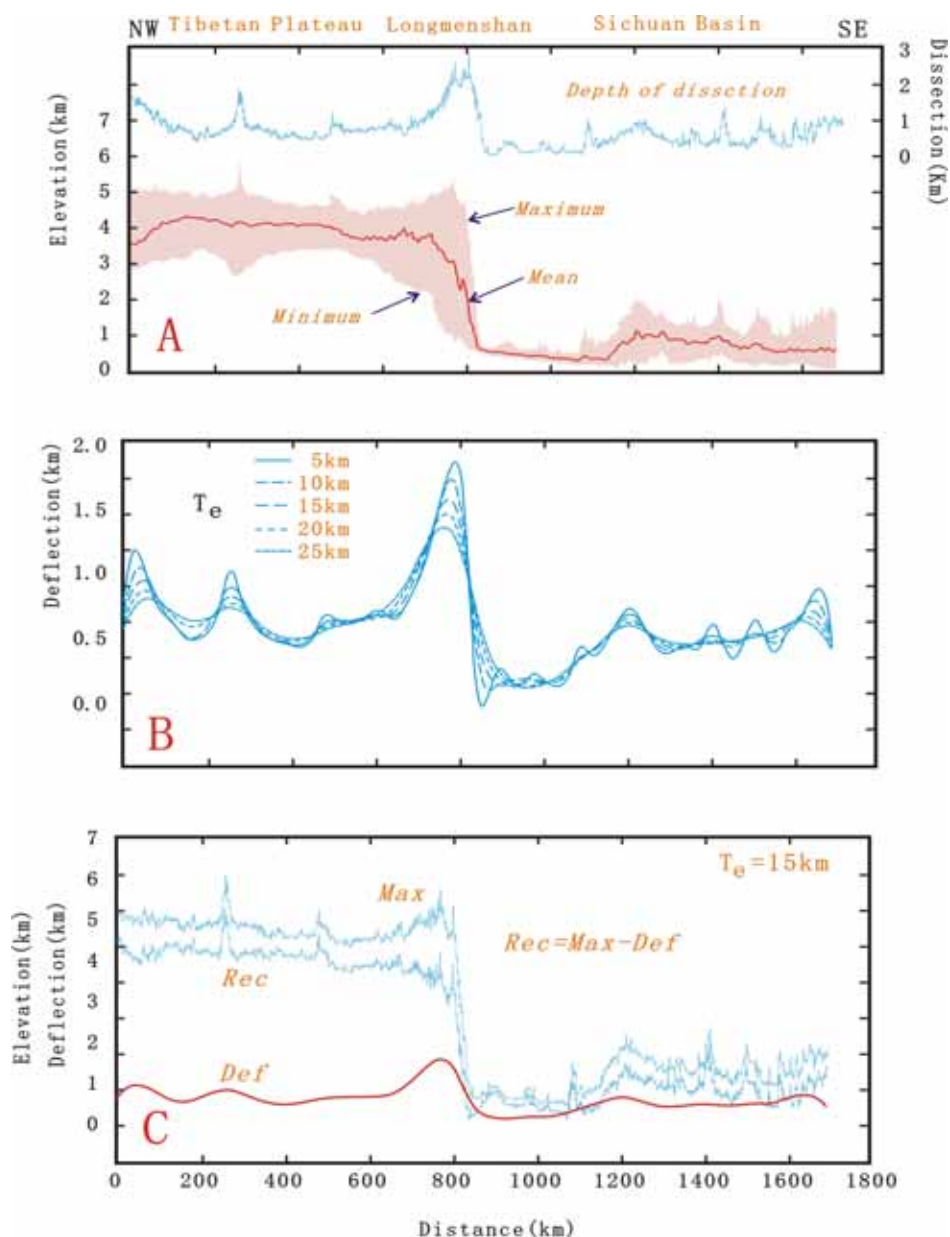


Figure 3 Elevation profiles along 1700 by 250 km swath across the Longmen Shan region from HYDRO1k data.

- A, mean elevations (Red line) calculated by every 1 km along the long axis of the swath. The gray area shows the maximum and minimum elevations. Note the rise in maximum elevations from the plateau (distances $x=0$ to 500 km) to the margin ($x=835$ km). The minimum profile marks the elevations of the river system that drains the region; it shows a curved profile within the plateau ($x=725$ to 835 km) and then slopes uniformly across the Sichuan Basin to the Yangtze River ($x=1180$ km). Depth of dissection (top curve) is the difference between the maximum and mean elevation profiles.
- B, deflection profiles calculated using eq.1 with different values of T_e . The load is given by the depth of dissection plus a small amount (<400 m) of Quaternary sediment between $x=835$ and 906 km (Burchfiel *et al.* 1995). Note that the deflection maximal and minima associated with the plateau margin migrate slightly away from the plateau with increasing T_e .
- C, reconstructed pre-erosion topography (Red) calculated by subtracting the deflection profile with $T_e=15$ km (Def) from the present maximum topography (Max). Note the decreased relief and gradient of the reconstructed topography at the margin. Also note the forebulge in the reconstructed Sichuan Basin at $x=910$ km, 75 km forward of the margin.

material eroded from the margin is now transported across and out of the foreland. This inferred eastward tilting is consistent with observations of Neogene(?) conglomerates near Dayi that now dip $\sim 20^\circ$ SE (Burchfiel *et al.* 1995).

6 Discussion

Details of the deflection profiles provide several testable predictions that could constrain an estimate of the average T_e in the Longmen Shan region. At high values of T_e , the positions of the deflection minimum in the Sichuan Basin migrate eastwards, away from the margin. The actual position of this minimum should be detectable in the geometry and tilts of river terraces in the basin and, because alluvial rivers are highly sensitive to slope, changing river platform sinuosity (e.g., Schumm 1986).

The long, dominantly strike-slip faults described here are consistent with tectonic models that invoke large-scale N-S dextral shear across the eastern Tibetan Plateau (England and Molnar, 1990), and are inconsistent with crustal extrusion models (Avouac and Tapponnier 1993). Erosional unloading is capable of producing significant and localized rock uplift along the margin, effectively exaggerating the form of any inherited mountain

front and creating the illusion of rapid upper crustal shortening. It is the reconstructed, pre-erosion topography that must therefore be explained in terms of crustal thickening or lower crustal flow. Clark and Royden (2000) used the present topography to estimate the viscosity of lower crustal material under the Tibetan Plateau and adjacent regions. Their analysis yielded viscosities of 10^{21} Pa s under a transect across the Longmen Shan region, 3–4 orders of magnitude higher than those under transects just to the north and south. It seems likely that a revised estimate of viscosity using the reconstructed, rather than the present, topography might be more similar to neighboring values.

Acknowledgments

The field work in China was supported by the NSF (EAR 9803484) to M. Ellis and A. Densmore, and NSFC (40372084), SZD0408 and EYTP to Li Yong. Accommodation and logistical support in China were kindly provided by Chengdu University of Technology. We thank Si Guanying and Melissa Swartz for their assistance in the field, and Eric Kirby and Philip Allen for helpful discussions.

References

- Avouac, J. P., and Tapponnier, P. 1993. Kinematic model of active deformation in central Asia. *Geophysical Research Letters* **20**: 895–898
- Burchfiel, B. C., CHEN, Z., LIU, Y., and Royden, L.H. 1995. Tectonics of the Longmen Shan and adjacent regions. *International Geology Review* **37**: 661–735
- CHEN, S.F., Wilson, C. J. L., DENG, Q.D., ZHAO, X.L., and LUO, Z.L. 1994. Active faulting and block movement associated with large earthquakes in the Min Shan and Longmen Mountains, Northeastern Tibetan plateau. *Journal of Geophysical Research* **99**: 24025–24038
- CHEN, S. F., and Wilson, C.J.L. 1996. Emplacement of the Longmen Shan Thrust-Nappe Belt along the eastern margin of the Tibetan Plateau. *Journal of Structural Geology* **18**: 413–430
- Clark, M.K., and Royden, L.H. 2000. Topographic ooze: building the eastern margin of Tibet by lower crustal flow. *Geology* **28**: 703–706
- Dirks, P. H. G. M., Wilson, C. J. L., CHEN, S., LUO, Z. L., and LIU, S. 1994. Tectonic evolution of the NE margin of the Tibetan Plateau: evidence from the central Longmen Mountains, Sichuan Province, China. *Journal of Southeast Asian Earth Sciences* **9**: 181–192
- England, P.C., and Houseman, G.A. 1986. Finite strain calculations of continental deformation: 2, comparison with the India-Asia collision zone. *Journal of Geophysical Research* **91**: 3664–3676
- England, P., and Molnar, P. 1990. Right-lateral shear and rotation as the explanation for strike-slip faulting in eastern Tibet. *Nature* **344**: 140–142
- Gilchrist, A.R., Summerfield, M.A., and Cockburn, H.A.P. 1994. Landscape dissection, isostatic uplift, and the morphologic development of orogens. *Geology* **22**: 963–966
- Hetenyi, R. 1974. *Beams on elastic foundation*: Ann Arbor. University of Michigan Press. Pp 255
- Holt, W.E. 2000. Correlated crust and mantle strain fields in Tibet. *Geology* **28**: 67–70
- King, G. C. P., and Ellis, M. 1990. The origin of large local uplift in extensional regions. *Nature* **348**: 689–693
- King, R. W., Shen, F., Burchfiel, B.C., Royden, L.H., Wang, E., CHEN, Z., LIU, Y., Zhang, X. Y., ZHAO, J. X., and Li, Y. 1997. Geodetic measurement of crustal motion in southwest China. *Geology* **25**: 179–182

- Kirby, E., Whipple, K. X., Burchfiel, B. C., Tang, W., Berger, G., Sun, Z., and CHEN Z. 2000. Neotectonics of the Min Shan, China: implications for mechanisms driving Quaternary deformation along the eastern margin of the Tibetan Plateau. *Geological Society of America Bulletin* **112**: 375~393
- Maggi, A., Jackson, J.A., McKenzie, D., and Priestley, K. 2000. Earthquake focal depths, effective elastic thickness, and the strength of the continental lithosphere. *Geology* **28**: 495~498
- McKenzie, D., and Farihead, D. 1997. Estimates of the effective elastic thickness of the continental lithosphere from Bouguer and free-air gravity anomalies. *Journal of Geophysical Research* **102**: 27523~27552
- Royden, L.H., Burchfiel, B.C., King, R.W., Wang, E., CHEN, Z., Shen, F., and LIU, Y. 1997. Surface deformation and lower crustal flow in eastern Tibet. *Science* **276**: 788~790
- Schumm, S.A. 1987. *Alluvial river response to active tectonics, in Studies in geophysics: Active tectonics*. Washington D.C., National Academy Press. Pp 80~94
- Stein, R. S., King, G.C.P., and Rundle, J. 1988. The growth of geologic structures by repeated earthquakes. 2, field examples of continental dip-slip faults. *Journal of Geophysical Research* **93**: 133319~133331
- WANG, E., Burchfiel, B. C., Royden, L. H., CHEN, L., CHEN, J., Li, W., and CHEN, Z. 1998. Late Cenozoic Xianshuihe-Xiaojiang, Red River, and Dali fault systems of southwestern Shichuan and central Yunnan, China. *Geological Society of America Special Paper* **327**: 1~108